Electronic Supplementary Material (ESI) for Journal of Materials Chemistry A.

Supporting information

Metal-doped bipyridine linked covalent organic framework films as a platform for photoelectrocatalysts

Tomoya Hosokawa, Masaki Tsuji, Kosei Tsuchida, Kazuyuki Iwase, Takashi Harada, Shuji Nakanishi, and Kazuhide Kamiya,**

Synthesis of 5,5'-Diamino-2,2'-bipyridine

5,5'-Diamino-2,2'-bipyridine (bpy) was synthesized on the basis of the previously reported method with slight modifications.[s1-2] All commercially available reagents and solvents were purchased and used as received without further purification.

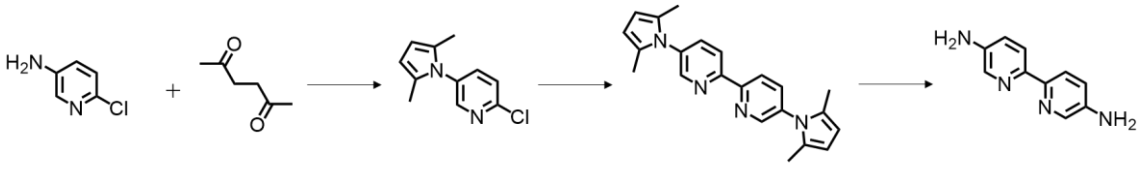

(1) (2) (3)

1-(2-Chloropyridine)-5-yl-2,5-dimethyl-1*H*-pyrrole (**1**)

5-Amino-2-chloropyridine (5.08 g) (TCI), 2,5-hexanedione (6 mL) (TCI), and amine-*p*-toluene sulfonic acid monohydrate salt (*p*-TsOH) (102 mg) (TCI) were dissolved in toluene (Wako) (80 mL) and heated at 133 °C in a Dean–Stark apparatus under stirring

for 5 h. After cooling to room temperature, the mixture was washed with saturated sodium hydrogen carbonate ($NaHCO_3$) (Wako) solution and brine (Wako) and dried over anhydrous magnesium sulfate ($MgSO_4$) (Wako) overnight. The resultant liquid was evaporated under reduced pressure, and a yellow solid was obtained. Yield: 7.95 g (97%). ^{1}H NMR (498 MH_Z, $CDCl_3$, 298 K): δ = 8.33 (d, *J* = 2.6 Hz, 1H) , 7.47–7.57 (m, 2H), 5.97 (s, 2H), 1.94–2.22 (m, 7H)

5,5'-Bis(2,5-dimethyl-1*H*-pyrrole)-2,2'-bipyridine (**2**)

Zinc powder (2.81 g) (TCI), which was pre-treated with hydrochloric acid (HCl) (35–37 wt.%, Wako), tetraethylammonium iodide (6.49 g) (TCI), and bis(triphenylphosphine)nickel(II) bromide (3.69 g) (Sigma-Aldrich) were suspended in tetrahydrofuran (THF) (10 mL) (anhydrous, TCI) and stirred at 55 °C under N_2 for 3 h. Compound **1** (5.22 g) dissolved in THF (30 mL) was slowly added to this mixture using a syringe, and the resultant mixture was stirred overnight. After cooling to room temperature, ammonia solution (100 mL) (25 wt.%, Wako), distilled water (50 mL), and dichloromethane (200 mL) (Wako) was added. After the combined solution was stirred for 15 min, the precipitate was filtered off, and the aqueous phase was extracted with small portions of dichloromethane. The combined organic phases were washed with brine and then evaporated under reduced pressure. The obtained crude compound (2.03 g) dissolved in dichloromethane (20 mL) was further purified by open column chromatography with *n*-hexane (Wako)/ethyl acetate (Wako)/trimethylamine (Wako) (10/1/0.05 v/v) as the eluent to afford the title compound as a light-yellow solid. Yield: 1.23 g (14%). ^{1}H NMR (498 MHz, $CDCl_3$, 298 K, TMS): δ = 8.60–8.62 (m, 2H, *J* = 5.6 Hz), 7.75 (dt, *J* = 8.3, 1.3 Hz, 1H), 6.00 (s, 2H), 2.00–2.26 (m, 5H)

5,5’-Diamino-2,2’-bipyridine (**3**)

Compound **2** (1.19 g), hydroxylamine hydrochloride (7.30 g) (Sigma-Aldrich), trimethylamine (4 mL) (Wako), ethanol (25 mL) (Wako), and distilled water (10 mL) were heated at 110 °C under reflux for 20 h. Another portion of hydroxylamine hydrochloride (7.31 g) and triethylamine (2 mL) was then added. The solution was further heated at 110 °C under reflux for 24 h and then quenched by being poured into an ice-cooled HCl solution (30 mL) (3 M). Ice-cooled ethanol (50 mL) was added to the resultant suspension of a yellow precipitate, and the mixture was kept in the ice buss for 3 h with stirring. The yellow precipitate was collected and washed with distilled water. Yield: 0.661 g (73.3%). ^{1}H NMR (498 MHz, d_6-DMSO, 298 K, TMS): δ = 8.01–8.06 (m, 2H), 7.38 (d, J = 7.4 Hz, 1H)

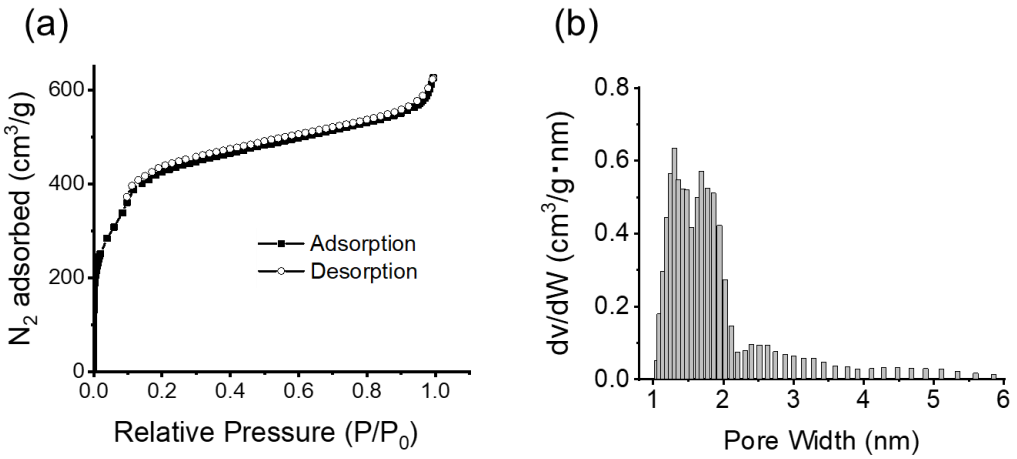

Figure S1. (a) Nitrogen adsorption–desorption isotherms of the ground bpy-COF films and (b) the pore size distribution calculated based on nonlocal density functional theory.

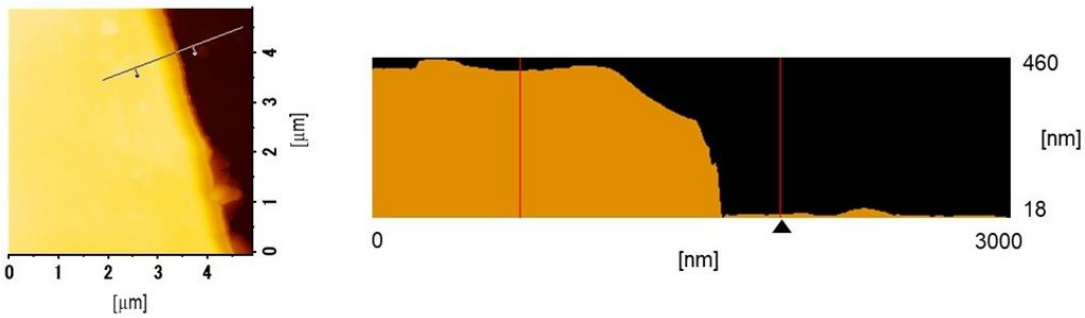

Figure S2. The AFM height image (left) and cross-section profile (right) of the 2D surfaces of the bpy-COF film.

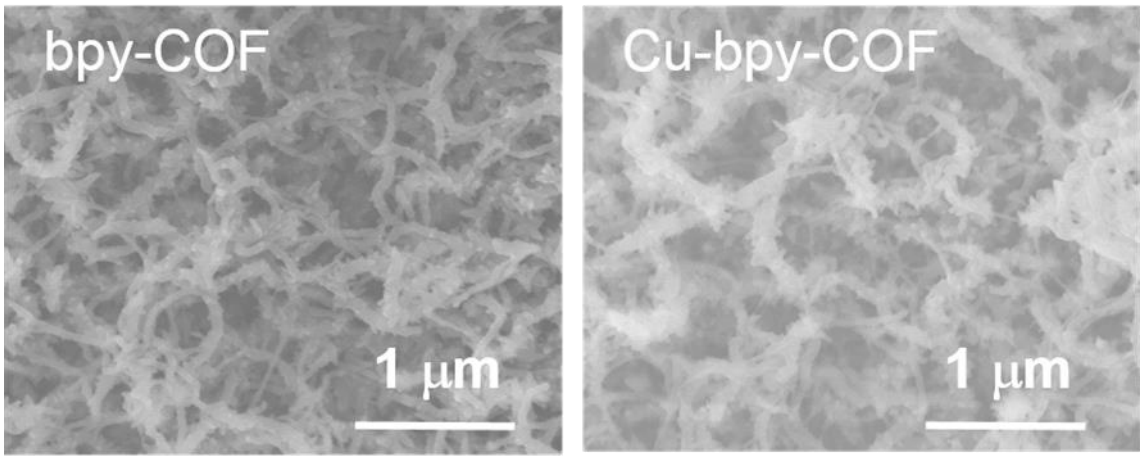

Figure S3. SEM micrographs of the bpy-COF(left) and the Cu-bpy-COF (right) film.

Table S1. Atomic composition of Cu-bpy-COF and bpy-COF films, as determined from XPS measurements (at%).

	Cu	C	O	N	Cl
Atomic concentration (%)	1.75	74	12	13	2.9

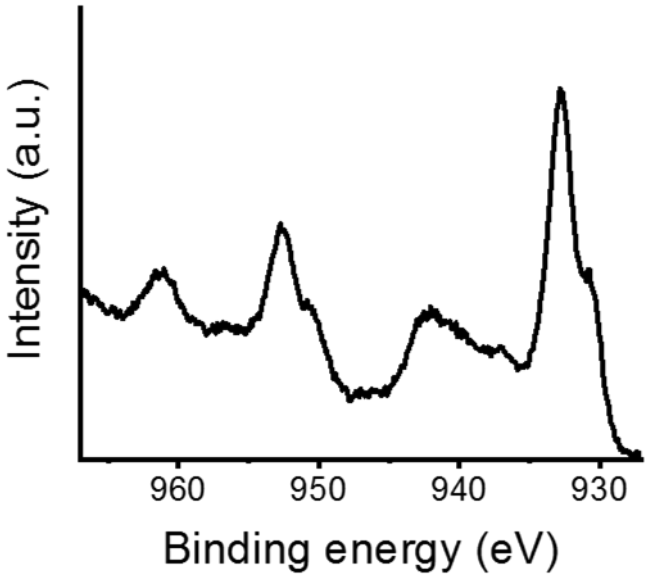

Figure S4. Cu 2p XPS spectra of Cu-bpy-COF films

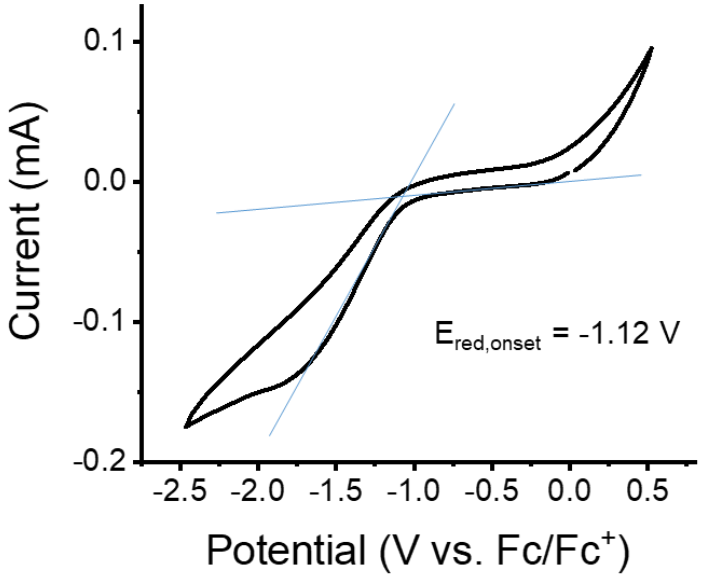

Figure S5. The *j* vs. *U* curves for a bpy-COF film on a glassy carbon electrode in an electrolyte composed of 0.1 M tetrabutylammonium hexafluorophosphate in acetonitrile. Scan rate = 50 mV s^{-1}.

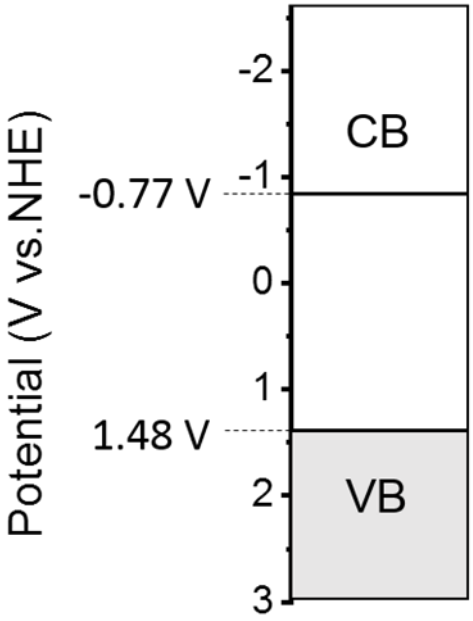

Figure S6. The proposed band structure of bpy-COF.

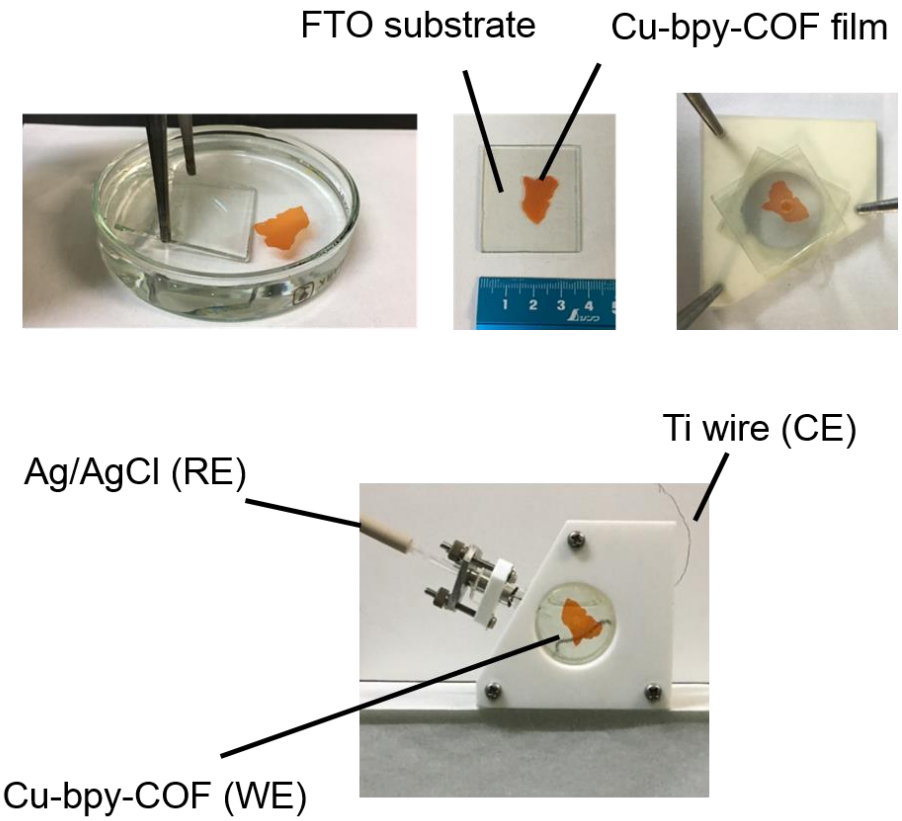

Figure S7. The preparation of the working electrode.

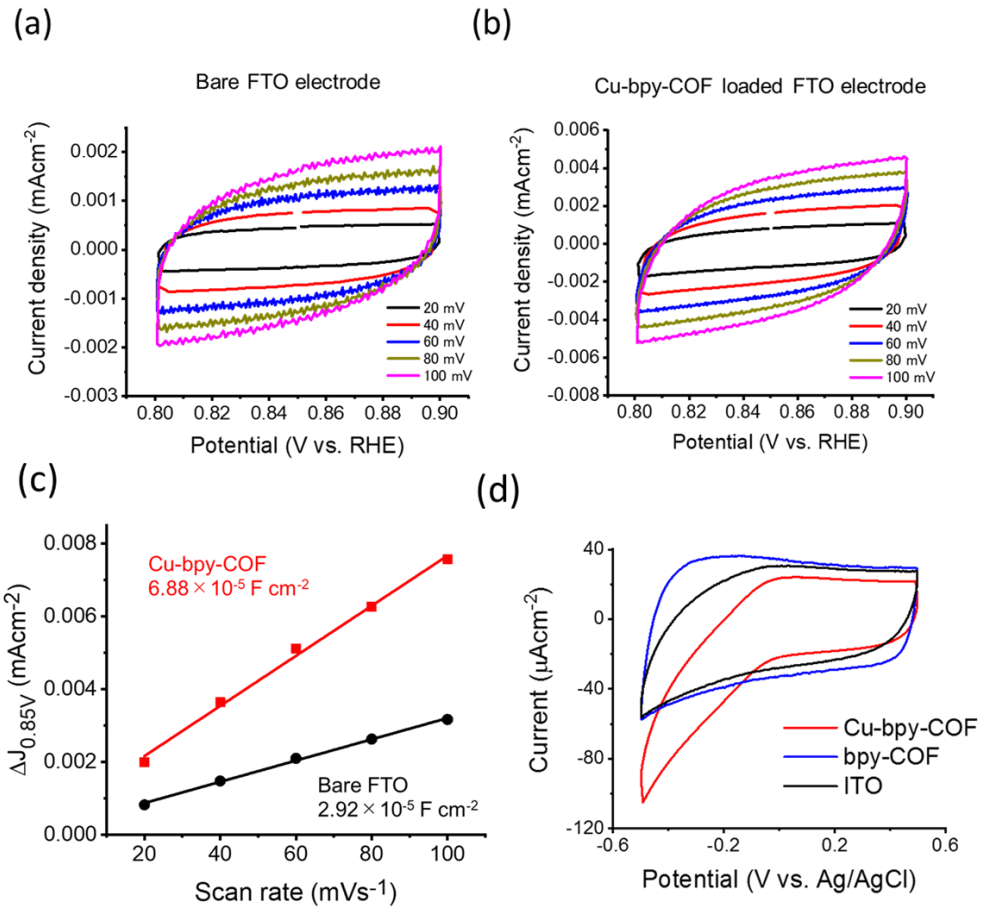

Figure S8. Cyclic voltammetry of (a) FTO and (b) Cu-bpy-COF at different scan rates in 0.1M phosphate buffer in the non-faradaic potential region. (c) Capacitive current density as a function of scan rate in the non-faradaic region (0.8 - 0.9 V vs. RHE) of the cyclic voltammograms for bare FTO (black) and Cu-bpy-COF loaded FTO electrode in 0.1 M phosphate buffer. (d) The *j* vs *U* curves under O_2 for Cu-bpy-COF (red), bpy-COF (blue), and ITO substrate (black) in phosphate buffer solution (pH 7). Scan rate = 100 mV s^{-1}.

Calculation of the electrochemically accessible surface area (EASA):

Cyclic voltammograms of the bare FTO electrode and Cu-bpy-COF loaded FTO electrode were recorded at different scan rates in the non-faradic region (Figure S8a and Sb). The double-layer capacitance was then calculated by the slope of the straight line of the capacitive current vs scan rates (Figure S8c). The double-layer capacitance of the bare FTO electrode was calculated to be $C_1 = 2.92 \times 10^{-5}$ F cm^{-2} and that of Cu-bpy-COF loaded FTO was $C_2 = 6.88 \times 10^{-5}$ F cm^{-2}.

The EASA of bare FTO electrode ($EASA_1$) has been calculated by running a cyclic voltammogram with 10 mM solution of $K_3[Fe(CN)_6]$ in 0.1 M pH 7 phosphate buffer solution using the Randles-Sevick equation (1):

$$i_p = 0.4463\, nFAC(nFvD/RT)^{\frac{1}{2}} \qquad (1)$$

where n is the number of electrons transferred (ferrocyanide, n = 1), F is the Faraday constant (96485 C mol^{-1}), A is the electrode area, C is the initial ferrocyanide concentration, v is the CV scan rate (0.05 V s^{-1}), R is the gas constant (8.314 J mol^{-1} K^{-1}) and T is the temperature (298 K). The diffusion coefficient (D) of ferrocyanide was based on the reference data (3.7×10 cm^2 s^{-1}).[s3]

Based on equation (1), $EASA_1$ is found to be 0.35 cm^2.

The EASA of the Cu-bpy-COF loaded FTO electrode ($EASA_2$) was calculated using the double-layer capacitance with following (2):

$$(EASA_1)/(EASA_2) = C_1/C_2 \qquad (2)$$

$EASA_2$ is calculated as 0.81 cm^2 using equation (2). The geometrical surface area of the electrode was 0.50 cm^2. The roughness factor for Cu-bpy-COF film calculated from $EASA_2$ (1.62) value is similar to the reported value for Co-bpy-COF powder electrode (1.44).[s4]

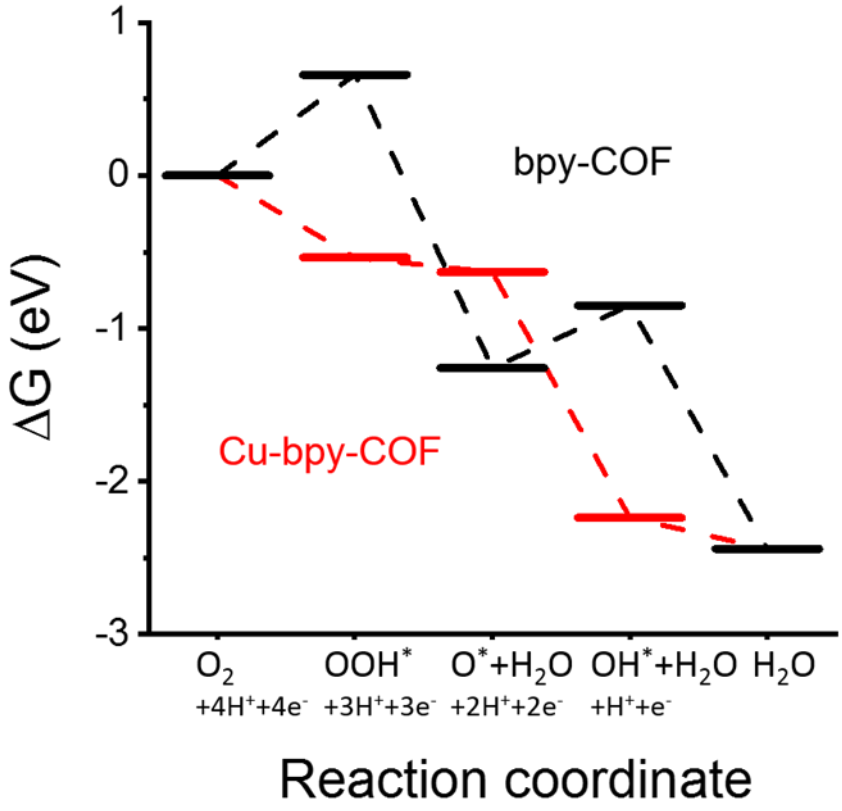

Figure S9. Free-energy diagram for each reaction coordinate for the ORR for Cu-bpy-COF (red) and (black) bpy-COF (electrode potential: 0.62 V vs. CHE).

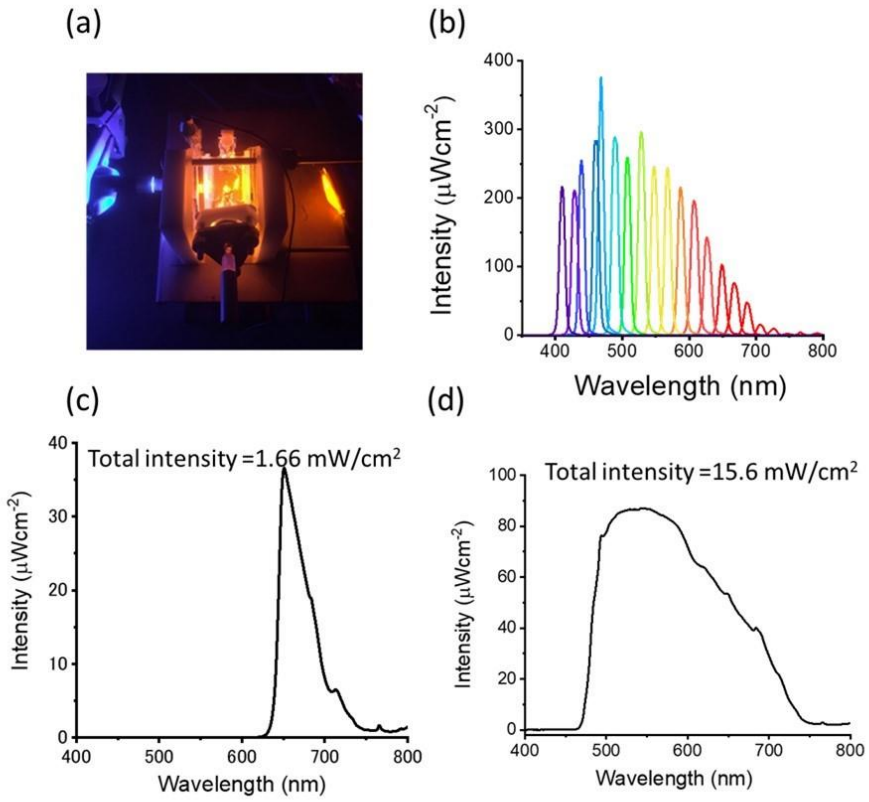

Figure S10. (a) The experimental setup was used for photocurrent measurements. (b) Irradiated spectra of the monochromated light used at the photocurrent measurements for Figures 4a and S11 (650 nm monochromated light with 1.36 mW/cm^2). The broad irradiated spectra were used at the photocurrent measurements (c) for Figure 4b and S13, and (d) for Figure S12.

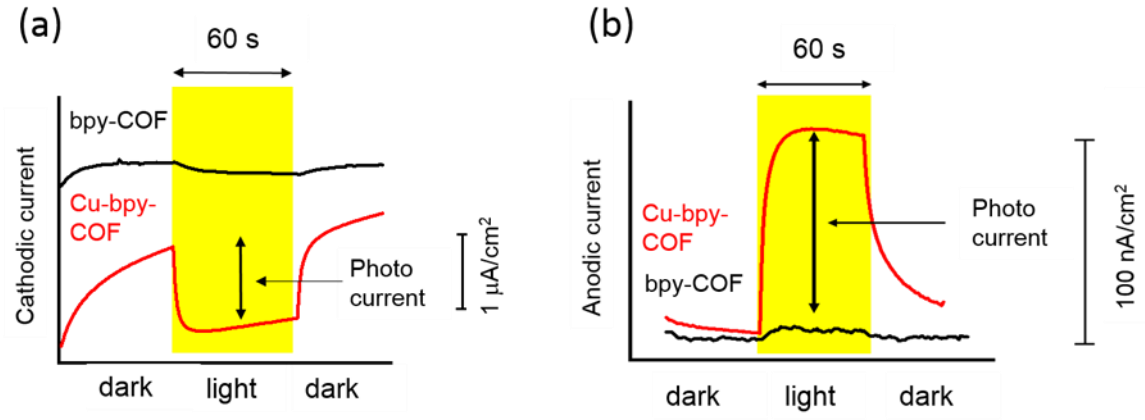

Figure S11. Photocurrent response for (red) Cu-bpy-COF and (black) bpy-COF at (a) −0.2 V and (b) +0.2 V vs. Ag/AgCl under illumination (The monochromated light at 650 nm was used as shown in Figure S10b). These photocurrent responses were measured under the constant potentials.

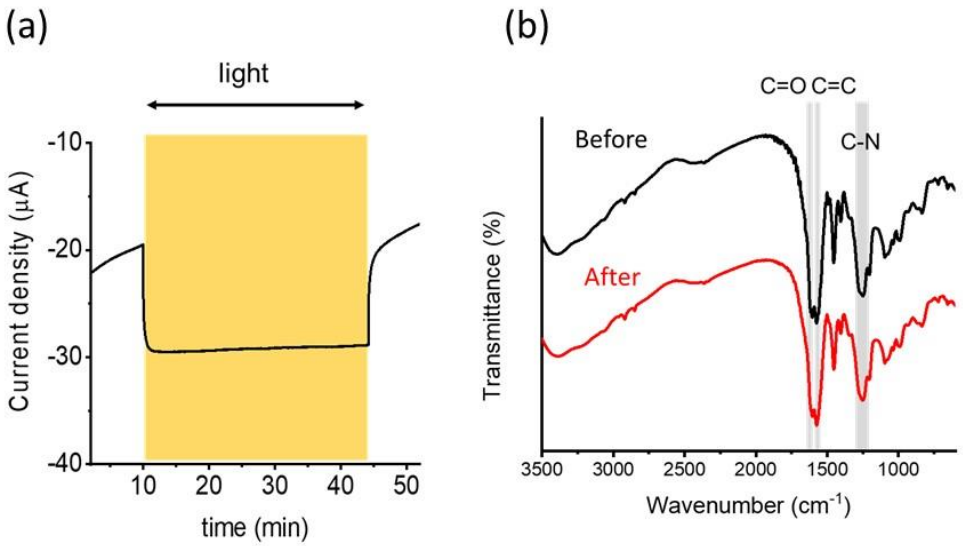

Figure S12. (a) Photocurrent response for Cu-bpy-COF for 35 min at –0.2 V vs. Ag/AgCl under illumination (The irradiated light is shown in Figure S10d). (b) FT-IR spectra of Cu-bpy-COF films before and after the photoelectrochemical test.

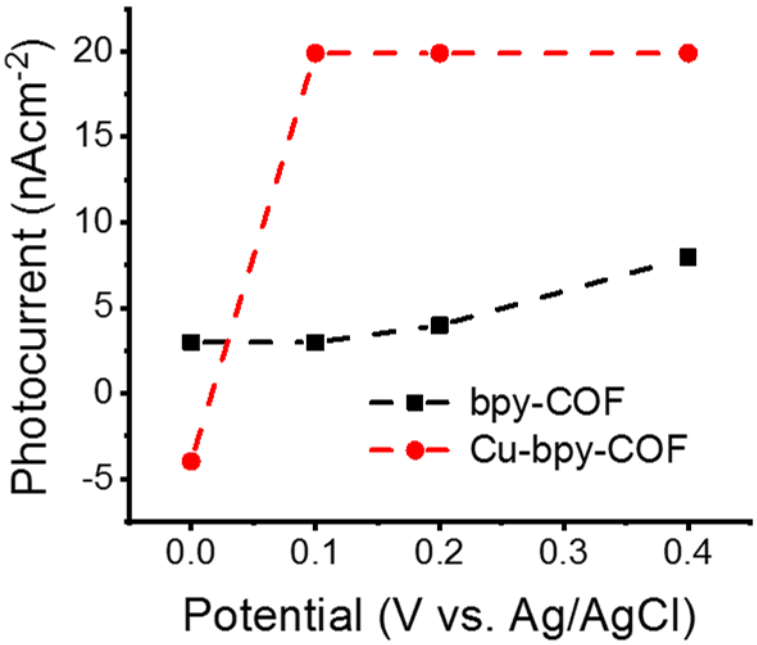

Figure S13. Potential dependence of the photocurrent for (red) Cu-bpy-COF and (black) bpy-COF under illumination (The irradiated light is shown in Figure S10c). These photocurrent responses were measured under constant potential.

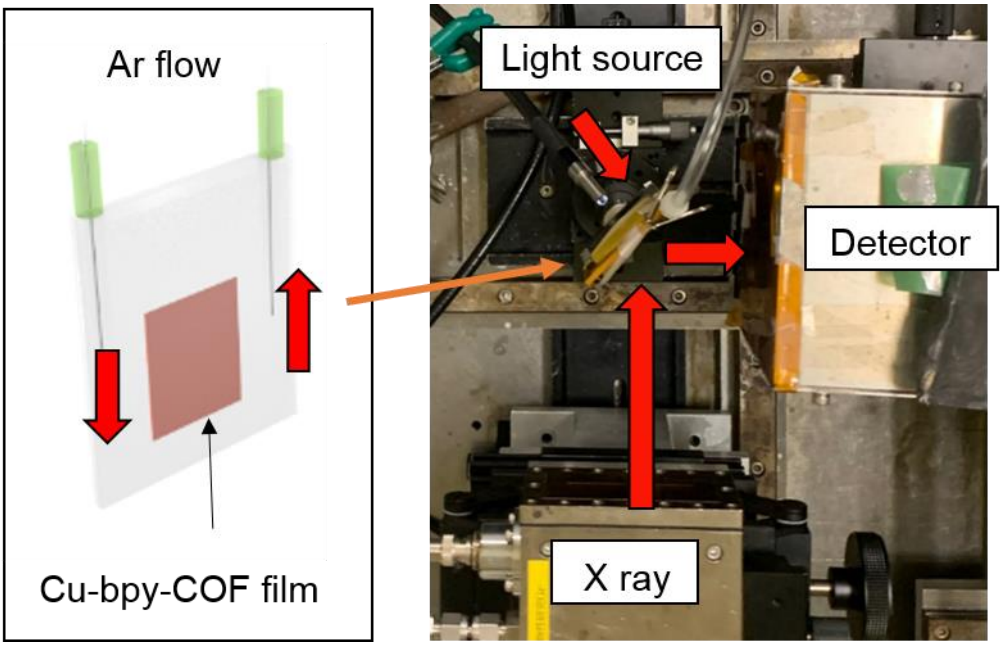

Figure S14. Schematic and photograph of the *in situ* XANES analysis system.

REFERENCES

[s1] M. Albrecht, I. Janser, A. Luetzen, M. Hapke, R. Froehlich, P. Weis, *Chem. Eur. J.* **2005**, *11*, 5742.

[s2] Q. Sun, B. Aguila, J. Perman, N. Nguyen, S. Ma, *J. Am. Chem. Soc.* **2016**, *138*, 15790.

[s3] Y.-X. Huang, X.-W. Liu, J.-F. Xie, G.-P. Sheng, G.-Y. Wang, Y.-Y. Zhang, A.-W. Xu and H.-Q. Yu, *Chem. Commun.*, 2011, **47**, 5795.

[s4] H. B. Aiyappa, J. Thote, D. B. Shinde, R. Banerjee and S. Kurungot, *Chem. Mater.*, 2016, **28**, 4375.